International Journal of Electrical Engineering and Technology.
ISSN 2249-3085 Volume 12, Number 1 (2022), pp. 25-48

http://www.ripublication.com

# A Modified Second Order Sliding Mode Control of Boost Inverter for Photovoltaic System

**B. Goldvin Sugirtha Dhas***

*Department of Electrical and Electronics Engineering,*
*Bannari Amman Institute of Technology, Sathyamangalam, India.*

**S.N. Deepa**

*Department of Electrical and Electronics Engineering, National Institute of Technology, Arunachal Pradesh, India.*

**Corresponding author. Ph. No. +91-9791737660.*

**Abstract**

This paper proposes a Modified Second Order Sliding Mode Control for boost inverter in photovoltaic system. The second order sliding mode can eliminate chattering caused by first order sliding mode control and also ensures high efficiency under system imperfection. A Lyapunov function is used to analysis the stability of the proposed controller. The proposed controller is compared with conventional controller. The comparison result substantiates that the second order sliding mode control gives fast response, less chattering and low Total Harmonic Distortion. The robustness of the controller is examined under different weather and load conditions respectively. The effectiveness of the proposed approach is demonstrated under MATLAB-SIMULINK environment.

**Keywords:** Modified Second Order Sliding Mode Control (MSOSMC), Sliding Mode Control (SMC), Boost Inverter and Photovoltaic (PV).

## 1. INTRODUCTION

With the continuous increasing cost of fossil fuels and the hazardous effect of using fossil fuels on the environment in the fields of power generation, transportation and industrial operation, the governments have moved towards the use of renewable sources

of energy by providing subsidies[1],[2]. The solar energy can provide clean technology and appropriate solution to the energy crisis admits all the renewable sources of energy. In the recent years, the photovoltaic system emerges as the important electrical power generating source in the world due to the improvement of efficiency and optimization of the Photovoltaic (PV) panels[3], [4]. In photovoltaic system, the power from the PV panel is transferred to load through converter/inverter and the transformer. Due to the advancement of power electronics in the recent year, the bulky and power consuming transformers are replaced by converters.

There are two types of converter configuration for photovoltaic system; one is single stage configuration and the other being two stage converter configuration. The single stage converters configuration is less efficient. Therefore, the photovoltaic system generally uses two stage converters to transfer the power from solar panel to the load. The first stage boosts the voltage from the PV and the second stage to convert the Direct Current (DC) voltage into Alternating Current (AC). However an efficient single stage converter derived from DC-DC converter which does both the operation in single stage is reported in[5]. This converter configuration is used in this paper for photovoltaic system as it has less number of components. The converters are usually non-linear in nature and it requires proper choosing or designing controller for its reliable operation. Several controlling techniques like P, PI, PID, Fuzzy logic, neural network controllers are proposed for the control of these converters[6].A two loop control was proposed in [7]. Among them, the Sliding Mode Control (SMC) is designed from non-linear control strategy and used to control non-linear system. The concepts of SMC is first reported to power electronics converter in [8].

The use of SMC is robust while it creates chattering in the output voltage. In [9], maximum power point tracking control utilizes a super twisting algorithm to eliminate chattering phenomenon for a system of relative degree one. The steady state response and transient response of the output voltage is improved in [10]by the modified SMC but it requires tuning of control parameters based on load variation. A two loop strategy with first loop to produce reference voltage for second loop to improve tracking of irradiance change was proposed in [11]with backstepping and sliding mode concepts for boost converter. in[12], the output voltage variation due to the input perturbations and the load disturbances are smoothened out using a super twisting differentiator-based high order SMC and is designed for step down converters.

The power loss due to variable switching frequency is eliminated in [13] for a Battery-supercapacitor hybrid energy storage system by a fixed frequency SMC in boost inverter while in [14], the fuzzy logic based dynamic SMC is applied for boost inverter in photovoltaic application with the output voltage having reduced Total Harmonic Distortion (THD). An adaptive control is designed in [15] for boost inverter with an autonomous oscillator for generating reference signal to avoid synchronization problems in grid connected systems. A double loop control is proposed in [16] for grid connected system which provides better performances under dynamic conditions. Ripple current is eliminated in [17]by a closed loop waveform control in boost inverter. In [18], a double loop control is proposed for boost inverter to remove dc offset and clipping effect. In [19], an adaptive super twisting SMC is applied to a boost inverter

for harmonic compensation and reactive power management. In [20], an adaptive fuzzy neural network control is adopted for the control of boost inverter with high learning ability and less knowledge of the plant while an adaptive fuzzy neural network control based on Total SMC was proposed in [21] for boost inverter. The phase shifted interleaved operation was proposed in [22] for battery-supercapacitor energy storage system to reduce the switching frequency current ripple component in it. High order smc based backstepping control was proposed in [23] to track the output voltage and to maintain the power factor close to one. [24]presented a SMC for injecting active power, grid current balance at unity power factor and load harmonics compensation while[25] proposed Observer-Based Higher Order SMC for Hybrid Electric Vehicle Applications to improve power factor in three-phase AC/DC converter.

The main motivation of this paper is to diminish the chattering effect and THD in the output voltage of the boost inverter. In this paper, a Modified Second Order SMC (MSOSMC) is proposed for boost inverter in photovoltaic system. The control consists of generation of reference voltage signal based on maximum power point tracking and the second loop is to track the reference maximum power point voltage and sinusoidal reference voltage.

The paper is organized as follows: The design of PV model in section 2. The mathematical model of boost inverter in section 3. The proposed MSOSMC followed by stability analysis in section 4. The simulation results are presented and discussed in section 5 and concludes in section 6.

## 2.PV MODEL

The two diode module with seven parameter deviate from the manufacturers' specifications [26] is the most accurate PV model with complex computation. Hence a two diode model [27]with four parameter is used and is depicted in Fig.1.The output equation of two diode model is

$$I = I_{PV} - I_0\left[\exp\left(\frac{V+IR_S}{V_T}\right)+\exp\left(\frac{V+IR_S}{(p-1)V_T}\right)-2\right]-\left(\frac{V+IR_S}{R_P}\right) \tag{1}$$

with:

$$I_{PV} = \left(I_{PV\_STC} + K_i\Delta T\right)\frac{G}{G_{STC}} \tag{2}$$

$$I_0 = \frac{\left(I_{PV\_STC} + K_i\Delta T\right)}{\exp\left[\left(V_{OC,STC} + K_v\Delta T\right)/\{a_1 + a_2/p\}V_T - 1\right]} \tag{3}$$

where,

$V_T=N_skT/q$

$\Delta T = T - T_{STC}(K)$

$T_{STC}$: Temperature at STC (25 $^0$C).

T: Temperature of the p–n junction (K).

$I_{PV\_STC}$: Light generated current at STC (A).

$K_i$: Short circuit currentcoefficient(°K).

G: Surface irradiance of the cell, and GSTC (1000 W/m$^2$).

$K_v$: Open circuit voltage coefficient.

$N_s$:Cells connectedin series.

q: Electron charge(1.60217646 ×10$^{-19}$C).

k:Boltzmann constant(1.3806503 ×10$^{-23}$J/K).

p: diffusion current(value chosen as 2.2).

$R_s$:Internal PV cell series resistance (Ω).

$R_p$:Internal PV cell parallel resistance (Ω).

p: The diode idealityconstant (p = 3).

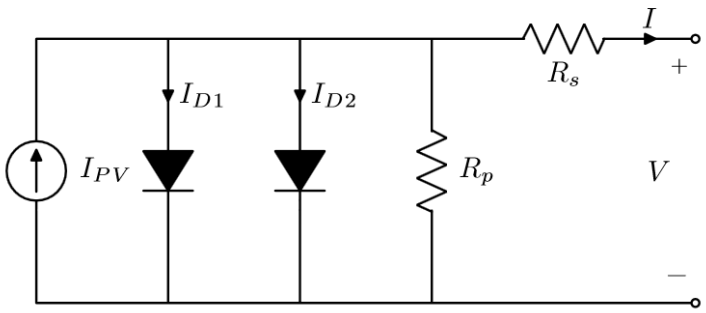


**Figure 1.**Two diode model of PV cell.

The power produced by the single cell is small. A number of PV cell is connected in series parallel combination to produce PV module of large power. Therefore the current equation is modified as

$$I = N_P\left\{I_{PV} - I_0\left[\exp\left(\frac{V + IR_SM}{V_T N_s}\right) + \exp\left(\frac{V + IR_SM}{(p-1)V_T N_s}\right) - 2\right] - \left(\frac{V + IR_SM}{R_P N_s}\right)\right\} \quad (4)$$

Where,

$$M = \frac{N_S}{N_P} \quad (5)$$

In this paper, the PV array consisting of two strings of five PV modules connected in series to produce a power of 1000 W. The electrical characteristics of commercially available SPR-E-Flex-100 PV module is given in the Table 1 and the I-V characteristics of SPR-E-Flex-100 PV module configured in 5 × 2 PV array is shown in the Figure 2.

**Table 1.** Electrical characteristics of the SPR-E-Flex-100 PV module at STC: 25° C, 1000w/$m^2$and AM-1.5.

| **Parameters** | **Value** |
|---|---|
| Nominal Power, $P_{mpp}$ | 100 W |
| Rated Voltage, $V_{mpp}$ | 17.1V |
| Rated Current, $I_{mpp}$ | 5.9 A |
| Open circuit voltage, $V_{oc}$ | 22.8 V |
| Short circuit current, $I_{sc}$ | 6.3A |
| Voltage Temp Coefficient, $K_v$ | –58.9 mV/° C |
| Temperature coefficient of voltage, $K_i$ | 2.6 mA/° C |
| Number of series cells, $N_s$ | 32 |

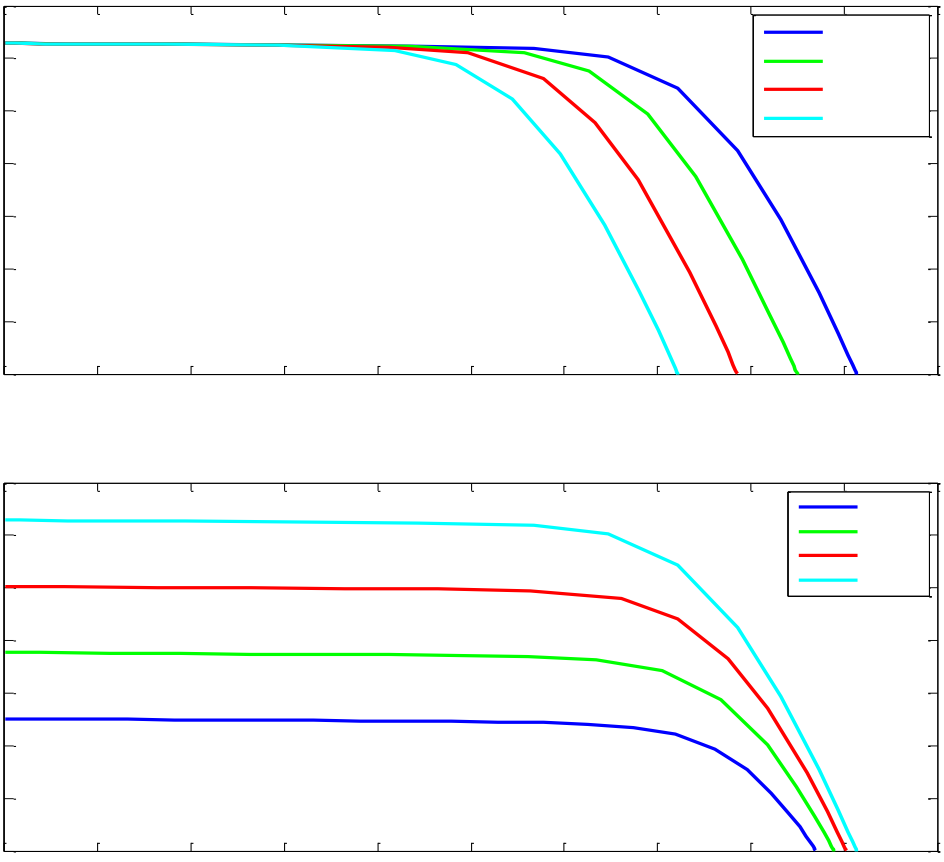

**Figure 2.** I–V characteristics curve for SPR-E-Flex-100 in 5×2 configuration for various temperature and irradiance.

## 3. BOOST INVERTER

In photovoltaic system, two stage converter are used for utilized for regulating and inverting the power from PV panel to the load[28]. In this paper, a boost inverter is considered which does the regulation and inversion in a single stage. The converter topology is presented in Fig. 3 where $V_{PV}$ is the PV cell input voltage, $V_0$ is the output voltage, $x_{1a}$ and $x_{1b}$ are the inductor current respectively and $x_{2a}$ and $x_{2b}$ are the voltage across the capacitors respectively. The inductor current is assumed to be PV current. The component L is the converter inductor, C is the converter's filter capacitor.

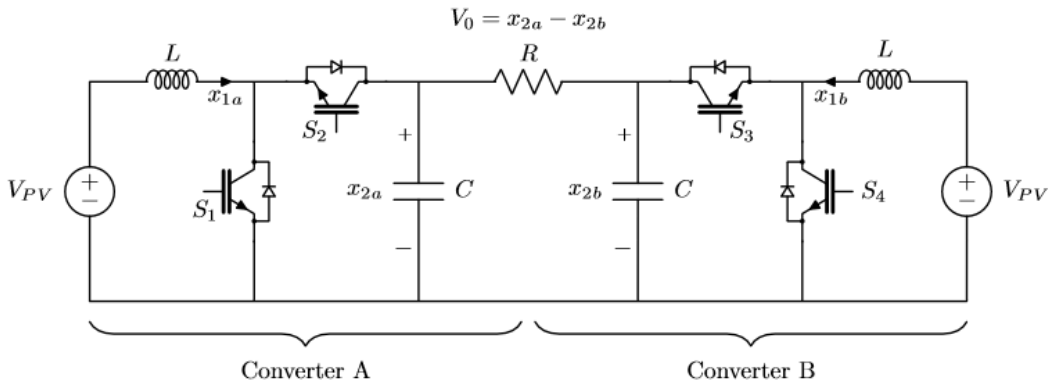


**Figure 3.** Boost inverter topology.

Since switches are used, there arises two switching states when

Case 1: Switches S1 and S4 are ON and S2 and S3 are OFF and

Case 2: Switches S1 and S4 are OFF and S2 and S3 are ON.

By applying Kirchhoff voltage law and Kirchhoff current law to the circuit under these two cases, a model for each switching position is obtained as follows,

Case 1:

$$\begin{cases} \dot{x}_{1a} = \dfrac{V_{PV}}{L} \\ \dot{x}_{2a} = -\dfrac{x_{2a} - x_{2b}}{RC} \\ \dot{x}_{1b} = \dfrac{V_{PV}}{L} \\ \dot{x}_{2b} = -\dfrac{x_{2b} - x_{2a}}{RC} \end{cases} \tag{6}$$

Case 2:

$$\begin{cases} \dot{x}_{1a} = \dfrac{V_{PV} - x_{2a}}{L} \\ \dot{x}_{2a} = -\dfrac{x_{2a} - x_{2b}}{RC} + \dfrac{x_{1a}}{C} \\ \dot{x}_{1b} = \dfrac{V_{PV} - x_{2b}}{L} \\ \dot{x}_{2b} = -\dfrac{x_{2b} - x_{2a}}{RC} + \dfrac{x_{1b}}{C} \end{cases} \tag{7}$$

Combining the equations of the both cases, we get

$$\begin{cases} \dot{x}_{1a} = \dfrac{V_{PV} - (1-u_a)x_{2a}}{L} \\ \dot{x}_{2a} = -\dfrac{x_{2a} - x_{2b}}{RC} + \dfrac{(1-u_a)x_{1a}}{C} \\ \dot{x}_{1b} = \dfrac{V_{PV} - (1-u_b)x_{2b}}{L} \\ \dot{x}_{2b} = -\dfrac{x_{2b} - x_{2a}}{RC} + \dfrac{(1-u_b)x_{1b}}{C} \end{cases} \tag{8}$$

Since both the converter circuits are identical, combining both the equation and rearranging, we get

$$\begin{cases} \dot{x}_1 = \dfrac{V_{PV}}{L} - \dfrac{x_2}{L}(1-u_a) \\ \dot{x}_2 = -\dfrac{x_2}{RC} + \dfrac{x_1}{C}(1-u_a) \end{cases} \tag{9}$$

with

$$x_2 = x_{2b} - x_{2a} \tag{10}$$

andsince the switches are complementary

$$u_a = 1 - u_b \tag{11}$$

Thegeneralized time invariant system given by

$$\dot{x} = f(t,x) + g(t,x)u \tag{12}$$

where

X= [I V] and u$\epsilon$ [0 1].

## 4. MODIFIED SECOND ORDER SLIDING MODE CONTROL

The output of each converter is

$$\begin{cases} x_{2a} = V_{dc} + V_m \sin(2\pi ft) \text{ and} \\ x_{2b} = V_{dc} + V_m \sin(2\pi ft - \pi) \end{cases} \quad (13)$$

The combined output is

$$x_2 = x_{2a} - x_{2b} = V_m \sin(2\pi ft) \quad (14)$$

There should be a pure sinusoidal output waveform at the output, so the switching policies are designed for $u_a$ and $u_b$ such that $x_2$ follows $x_{2ref}$given by,

$$x_{2ref} = V_m \sin(2\pi ft) \quad (15)$$

where

$V_m$ = Amplitude of the required AC voltage.

ω = Frequency of the required AC voltage.

To meet out the above condition, a MSOSMC is proposed. The MSOSMC is of second order to reduce the chattering and THD respectively. The SMC is implemented as choosing of the desired sliding surface and the choosing of the control law.

### 4.1 Controller design

Let us consider the surface

$$S_1 = K_1(x_2 - x_{2ref}) + K_2(V_{PV} - V_{ref}) \quad (16)$$

where,

$$V_{ref} = V_{in}(1\text{-}d(k)) \quad (17)$$

and d(k) is the duty cycle given in [29]is used and is given by

$$d(k) = d(k\text{-}1) \pm M \frac{dP}{dV} \quad (18)$$

Then the model can be written as

$$\dot{S}_1 = S_2 = K_1\left(-\frac{x_2}{RC} + \frac{(1-u_a)x_1}{C}\right) \quad (19)$$

$$\dot{S}_2 = -\frac{1}{RC}\left(-\frac{x_2}{RC} + \frac{(1-u_a)x_1}{C}\right) + \frac{(1-u_a)}{C}\left(\frac{V_{PV}}{L} - \frac{(1-u_a)x_2}{C}\right) \quad (20)$$

$$\dot{S}_2 = -\frac{(1-u_a)}{RC^2}x_1 - \left(\frac{(1-u_a)^2}{C^2} - \frac{1}{R^2C^2}\right)x_2 + \frac{V_{PV}}{LC}(1-u_a) \quad (21)$$

$$\dot{S}_2 = f(t,x) + g(t,x)u_a \tag{22}$$

where

$$f(t,x) = -\frac{(1-u_a)}{RC^2}x_1 - \left(\frac{(1-u_a)^2}{C^2} - \frac{1}{R^2C^2}\right)x_2 \tag{23}$$

$$g(t,x) = \frac{V_{PV}}{LC}(1-u_a) \tag{24}$$

This equation is of the form

$$\ddot{\sigma} = f(t,x) + g(t,x)u, f = \ddot{\sigma}|_{u=0}, g = \frac{\partial}{\partial u}\ddot{\sigma} \neq 0 \tag{25}$$

where f(t,x) and g(t,x) are unknown functions.

Assume that:

$$0 < K_m \leq g \leq K_M, |f| \leq F, F > 0 \tag{26}$$

Then equation (25) and (26) implies that

$$\ddot{\sigma} \in [-F, F] + [K_m, K_M]u \tag{27}$$

Therefore the problem can be stated as

$$u = \varphi(\sigma, \dot{\sigma}) \tag{28}$$

### 4.2. Controller design

The control law is defined as follows:

$$u = \begin{cases} 1, \text{if } \sigma > 0 \\ 0, \text{if } \sigma < 0 \end{cases} \tag{29}$$

This equation will trigger the switching across σ but the converter system has operating frequency limitation and chattering effect [30]. Hence the practical law can be restated as,

$$u = \begin{cases} 1, \text{if } \sigma > \gamma \\ 0, \text{if } \sigma < \gamma \end{cases} \tag{30}$$

where γ is a small positive number. From (14), it can be seen that the chattering effect is reduced as the chattering frequency across is σ reduced. It can also be expressed as,

$$u = \frac{1}{2}(1+\sigma) \tag{31}$$

A MSOSMC based on convergence law is defined as

$$\sigma = -sign\left(\beta \mid S \mid^{1/2} \; sign\, S\right) - k\int S \tag{32}$$

And

$$Km - F > \frac{\beta^2}{2} \tag{33}$$

where

α and β are constants, k is the integral constant, α >0, β> 0 and k > 0.The integral term is added to bring up better performance of the output voltage under closed loop condition [10].

### 4.3. Stability analysis

The Lyapunov function provides the sufficient condition to ensure the stability and the existence of finite-timeconvergence for a closed loop system. Therefore, the Lyapunov function is chosen as

$$V(t) = \frac{1}{2}S^2 \tag{34}$$

With

$$\begin{cases} V(0) = 0 \\ V(t) > 0 \text{ for } S(t) \neq 0 \\ \dot{S}(t) \neq 0 \end{cases} \tag{35}$$

The stability is achieved when

$$\begin{cases} \dot{V}(t) < 0 \\ S(t) \neq 0 \\ \dot{S}(t) \neq 0 \end{cases} \tag{36}$$

The derivative of the chosen surface is

$$\dot{S}_1 = K_1\left(-\frac{x_2}{RC} + \frac{(1-u_a)x_1}{C}\right) \tag{37}$$

Substituting the value of $u_a$,

$$\dot{S}_1 = K_1\left(-\frac{x_2}{RC} + \frac{x_1}{C}\left(1 - \left[\frac{1}{2}\left(1 - sign\left(\beta \mid S \mid^{1/2} \; sign\, S\right) - k\int S\right)\right]\right)\right) \tag{38}$$

$$\dot{S}_1 = K_1\left(-\frac{x_2}{RC} + \frac{x_1}{C}\left(\frac{1}{2} - sign\left(\beta \mid S \mid^{1/2} \; sign\, S\right) - k\int S\right)\right) \tag{39}$$

and

$$S_1\dot{S}_1 = S_1K_1\left(-\frac{x_2}{RC}+\frac{x_1}{C}\left(\frac{1}{2}-sign\left(\beta\mid S\mid^{1/2}\ sign\ S\right)-k\int S\right)\right) \quad (40)$$

From this equation (41), we can conclude that the stability is ensured as the derivative of the Lyapunov functionis negative and the required conditions of equation (37).

## 5. RESULTS AND DISCUSSION

The designed closed loop control of boost inverter in PV application in Matlab-Simulink is as shown in Figure 4. The proposed MSOSMC for Boost Inverter is tested and analysed for its applicability in photovoltaic system. The specification of boost inverter is given in the following Table 2. The PV system is usually affected by change in irradiance and change in load. The performance of the proposed control is tested under

i) Normal operation

ii) Changing irradiance

iii) Change in load

iv) Change in non-linear load

Furthermore, to evaluate the effectiveness of the proposed control, it is compared with the conventional dynamic SMC method[31]with the control parameter of $K_P$ =3.125e$^{-6}$and $K_I$ = 0.25.

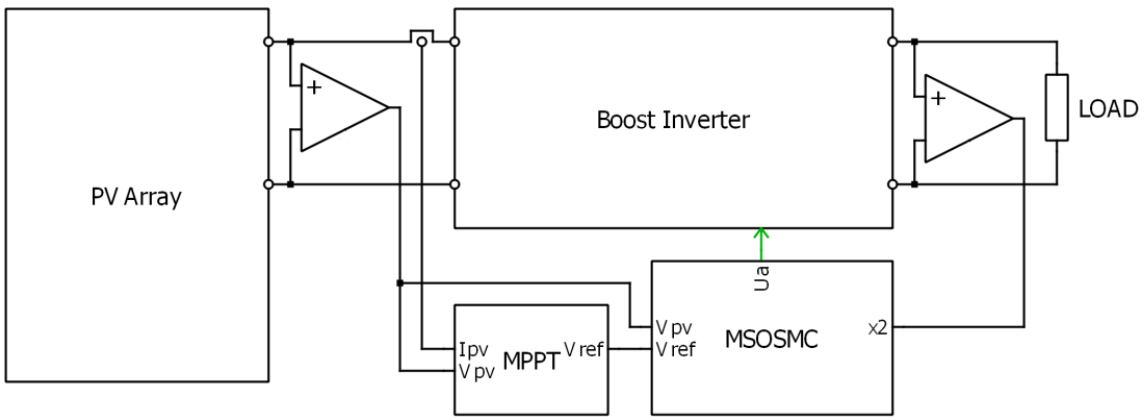


**Figure 4.** Closed loop control of boost inverter for PV application.

**Table 2.**Specifications of the boost inverter.

| Parameters | Range |
|---|---|
| Input voltage,$V_{in}$ | 60~120V |
| Rated output voltage, $V_0$ | 240V |
| Rated output power, $P_0$ | 1000W |
| Switching frequency, $f_s$ | 20kHz |
| Duty cycle, D | 0.3-0.71 |
| Inductance, $L_1$ | 180 µH |
| Capacitance, $C_1$ | 200 µF |
| Load, R | 57.6 Ω |

### 5.1 Normal operation at STC

The normal operation of PV system with MSOSMC and DSMC of Boost Inverter respectively is shown in Figure 5 and Figure 6. Figure5(a) shows the input voltage, capacitor voltages and output voltage for MSOSMC of Boost Inverter. Figure5(b) shows the PV current, inductor currents and the load current for MSOSMC of Boost Inverter.Figure5(c) shows the comparison of output voltage with the reference voltage for MSOSMC of Boost Inverter. Figure6(a) shows the input voltage, capacitor voltages and output voltage for DSMC of Boost Inverter. Figure6(b) shows the PV current, inductor currents and the load current for DSMC of Boost Inverter. Figure6(c) shows the comparison of output voltage with the reference voltage for DSMC of Boost Inverter.

From the Figure5, it can be seen that the MSOSMC provides less chattering in the capacitor voltages and the output voltage (Figure 5(a)), low ripple in inductor current and output current (Figure 5(b)) and it correctly tracks the reference voltage and has low THD (Figure 5(c)). While from the Figure 6, it can be seen that the chattering is high in capacitor voltages and the output voltage (Figure 6(a)), ripples is high in inductor current and output current (Figure 6(b)). Also DSMC has delayed tracking in the output voltage and higher THD in the output voltage (Figure 6(c)).

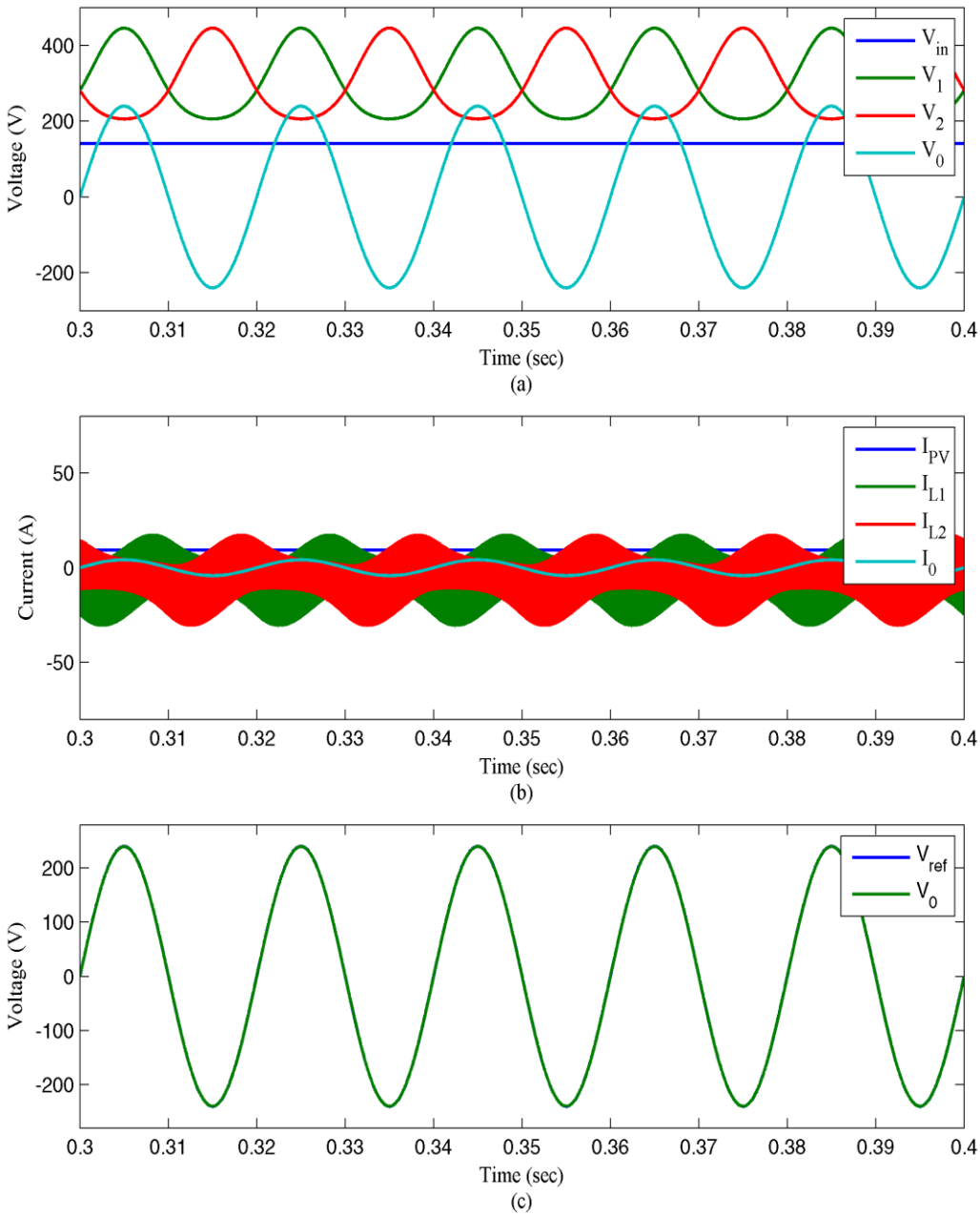


**Figure 5.** Normal operation of boost inverter controlled by MSOSMC. . (a) PV voltage, capacitor voltages, output voltage, (b) PV current, inductor currents and load current (c) The comparison of output voltage with the reference voltage.

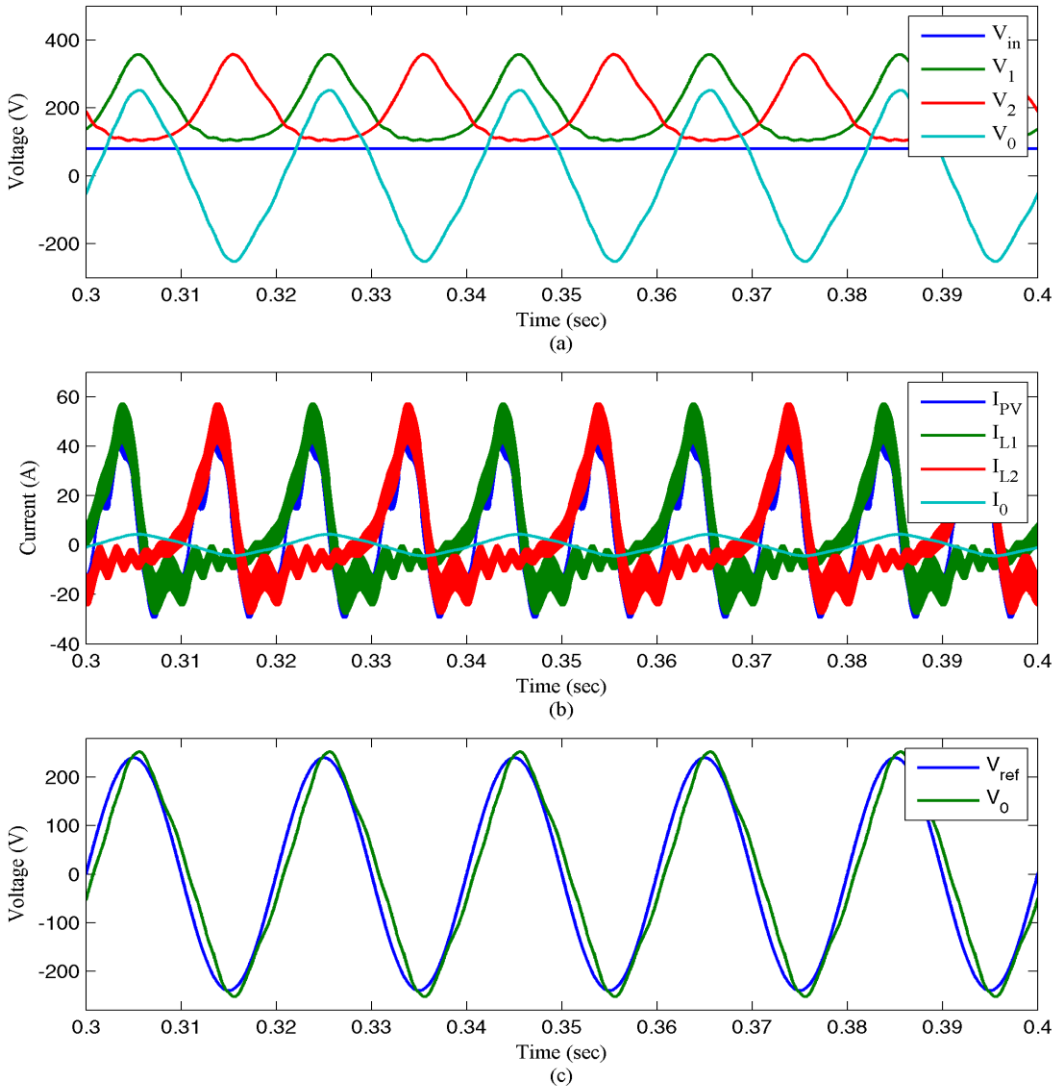


**Figure 6.** Normal operation of boost inverter controlled by DSMC. . (a) PV voltage, capacitor voltages, output voltage, (b) PV current, inductor currents and load current (c) The comparison of output voltage with the reference voltage.

### 5.2 Change in irradiance

In order to test the PV system under changing irradiance, the irradiance is changed from 500 W/m$^2$ to 1000W/m$^2$ at t = 0.325 s. Figure7 and Figure8 shows the PV system under change in irradiance with MSOSMC and DSMC respectively. From the Figure7, it can be seen that the MSOSMC provides less chattering and it correctly tracks the reference voltage (Figure 7(c)). While from the Figure 8, it can be seen that when the irradiance is low, the chattering is high in capacitor voltages and the output voltage (Figure 8(a)), ripples is high in inductor current and output current (Figure 8(b)). Also DSMC has delayed tracking in the output voltage (Figure 8(c)).

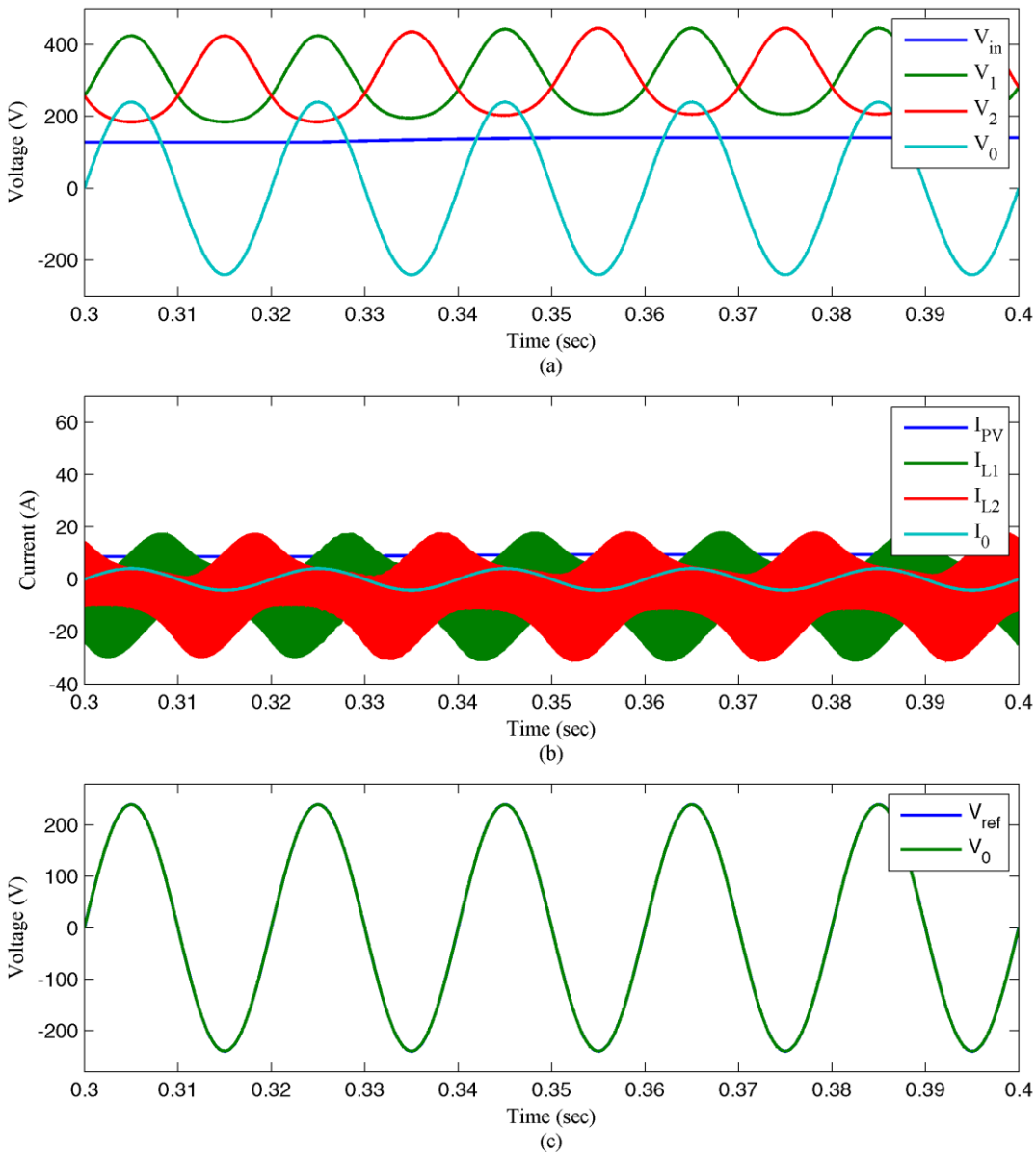


**Figure 7.** Normal operation of boost inverter controlled by MSOSMC under change in irradiance. . (a) PV voltage, capacitor voltages, output voltage, (b) PV current, inductor currents and load current (c) The comparison of output voltage with the reference voltage.

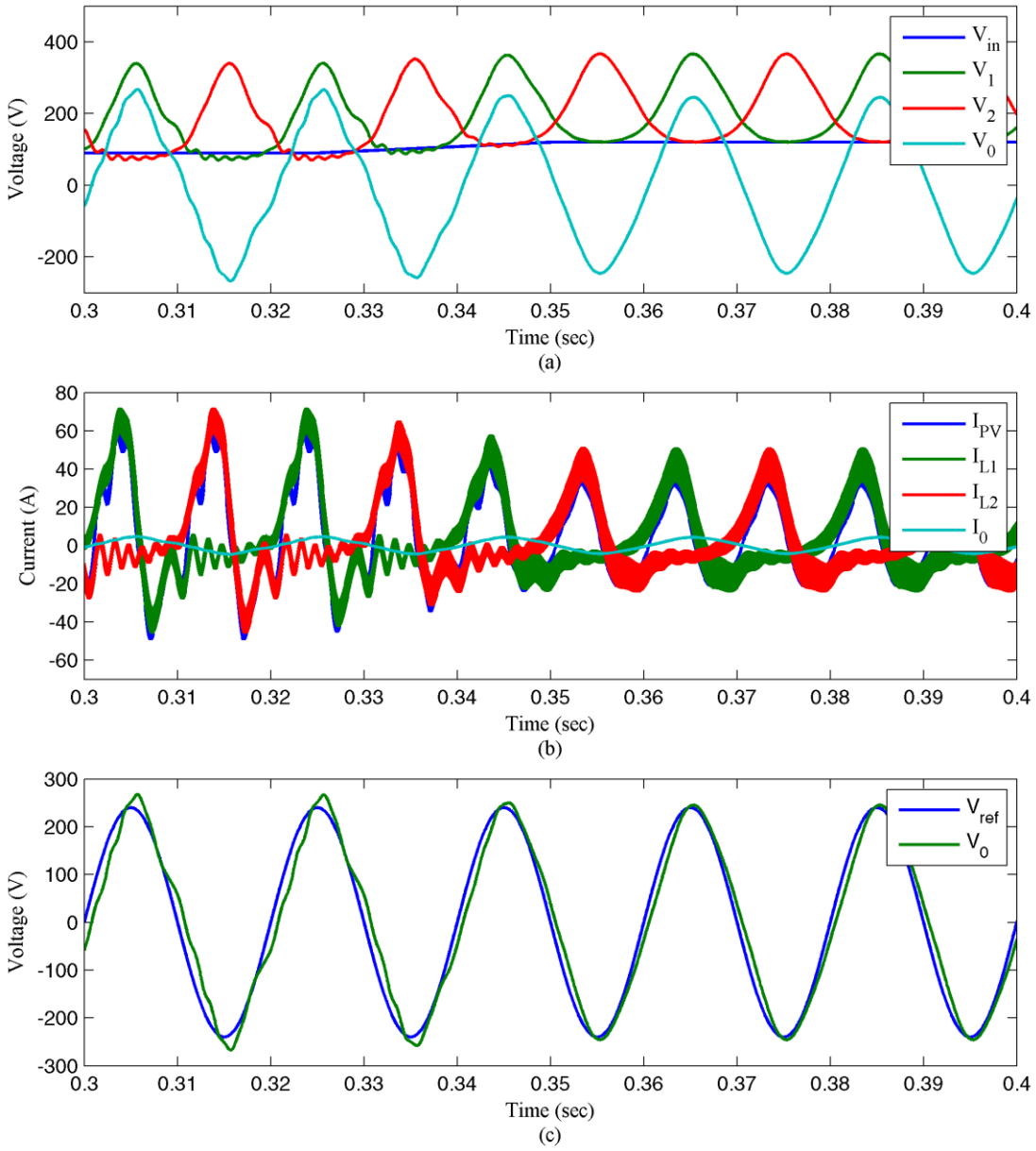


**Figure 8.** Normal operation of boost inverter controlled by DSMC under change in irradiance. (a) PV voltage, capacitor voltages, output voltage, (b) PV current, inductor currents and load current (c) The comparison of output voltage with the reference voltage.

### 5.3 Change in linear load

In order to test the PV system under change in linear load, the load is changed from 57.6 Ω to 28.8 Ω at t = 0.325 s. Figure 9 and Figure10 shows the PV system under change in linear load with MSOSMC and DSMC respectively. From the Figure 9, there

is a small oscillation in output voltage (Figure 9 (a)) and inductor current for half cycle respectively (Figure 9(b)). Also the MSOSMC provides less chattering and it correctly tracks the reference voltage (Figure 9(c)). While from the Figure 10 it can be seen that at the time of load change upto two cycles, the oscillation is high in capacitor voltages and the output voltage (Figure 10(a)), ripples is high in inductor current and output current (Figure 10(b)). Also DSMC has delayed tracking in the output voltage (Figure 10(c)).

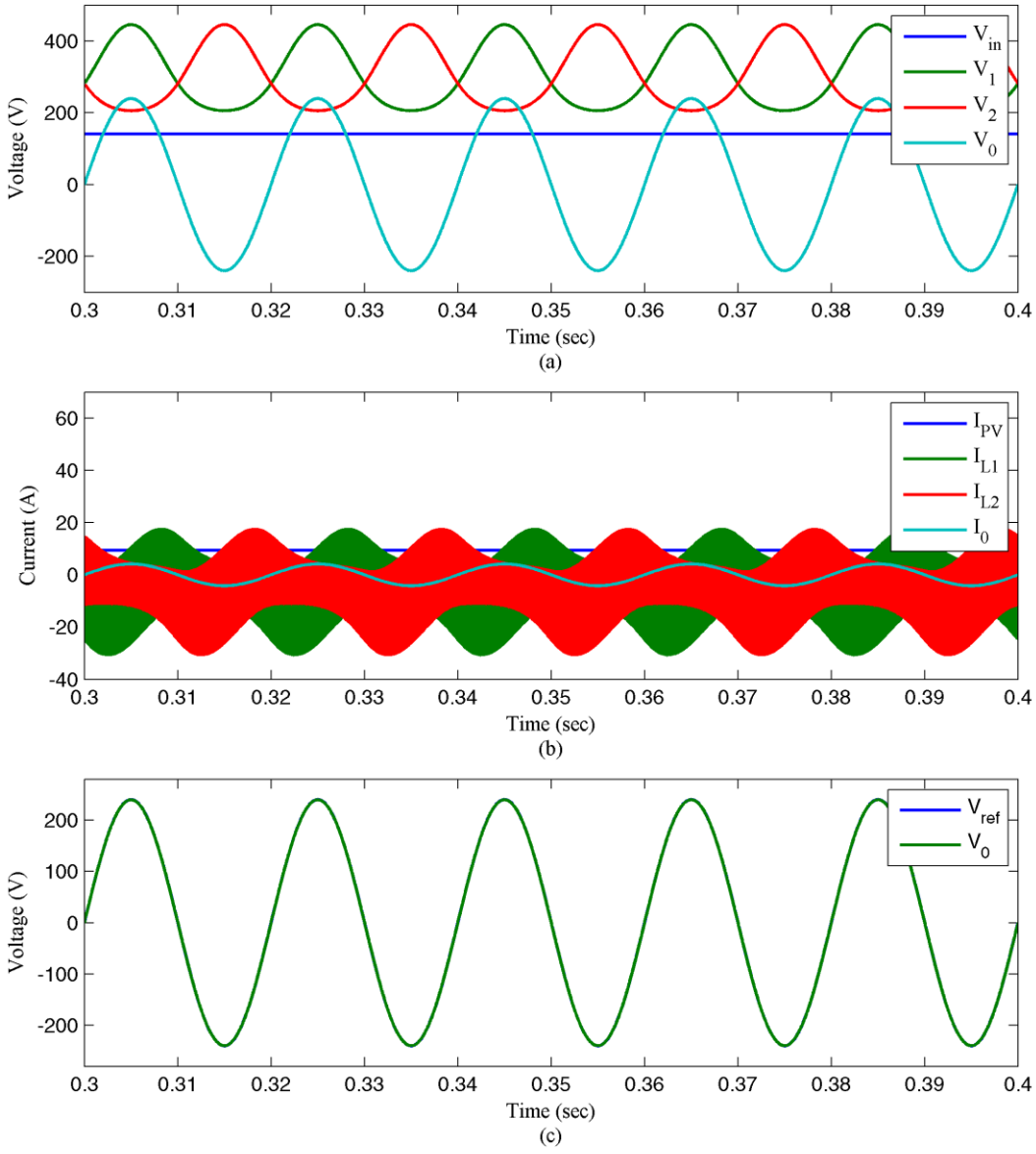


**Figure 9.** Normal operation of boost inverter controlled by MSOSMC under change in load. (a) PV voltage, capacitor voltages, output voltage, (b) PV current, inductor currents and load current (c) The comparison of output voltage with the reference voltage.

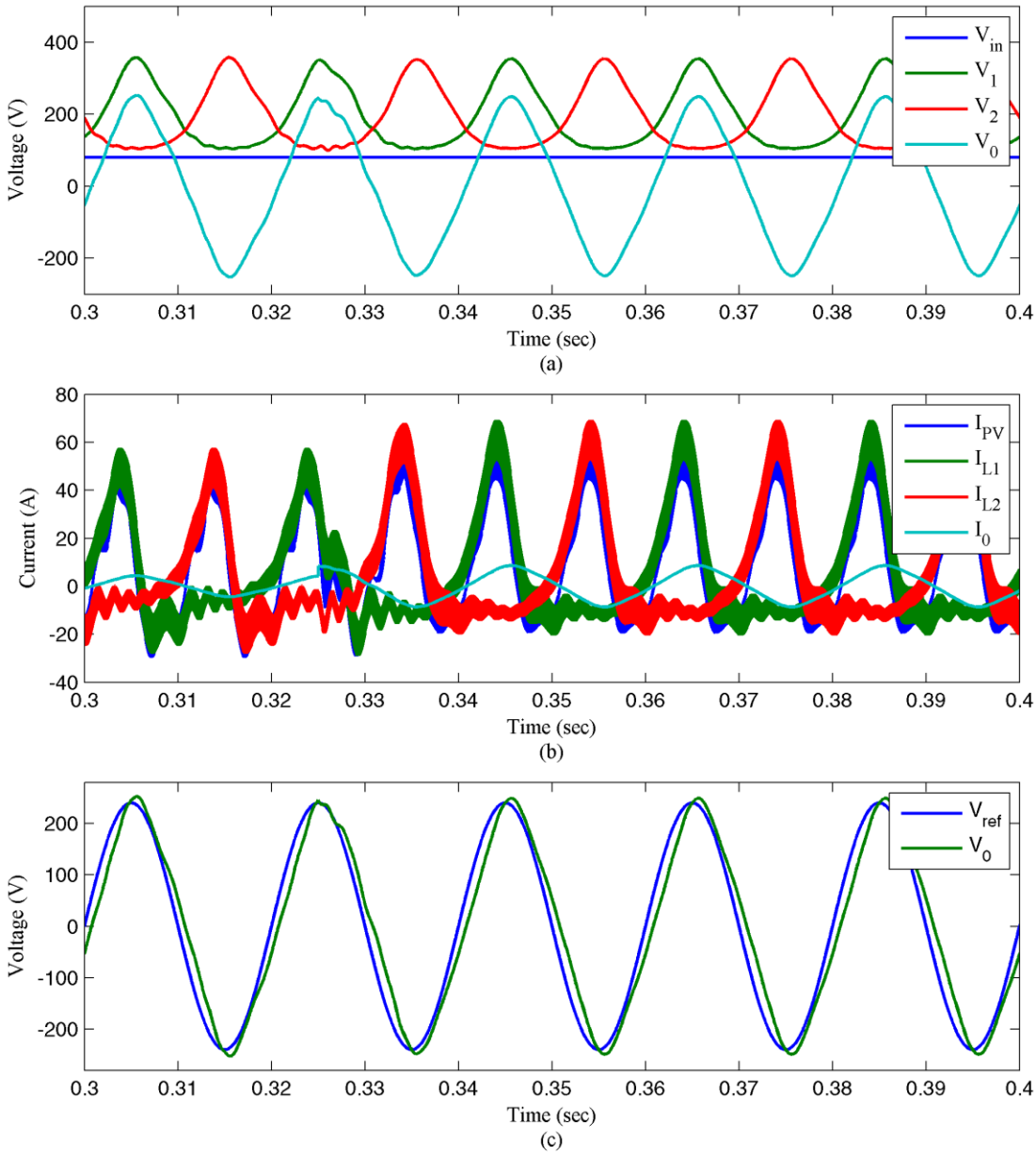


**Figure 10.** Normal operation of boost inverter controlled by DSMC under change in load. . (a) PV voltage, capacitor voltages, output voltage, (b) PV current, inductor currents and load current (c) The comparison of output voltage with the reference voltage.

### 5.4 Change in non-linear load

In order to test the PV system under change in non-linear load, the load is changed from R = 57.6 Ω to R = 57.6 Ω&100μHat t = 0.35 s. Figure 11 and Fig. 12 shows the PV system under change in non-linear load with MSOSMC and DSMC respectively. From

the Figure11, it can be seen that there is an increase ripple inductor current (Figure 11(b)) but the MSOSMC provides less chattering and it correctly tracks the reference voltage (Figure 11(c)). While from the Figure 12, it can be seen that at the time of load change upto three cycles, the oscillation is high in capacitor voltages and the output voltage (Figure 12(a)), ripples is high in inductor current and output current (Figure 12(b)). Also DSMC has delayed tracking in the output voltage (Figure 11(c)).

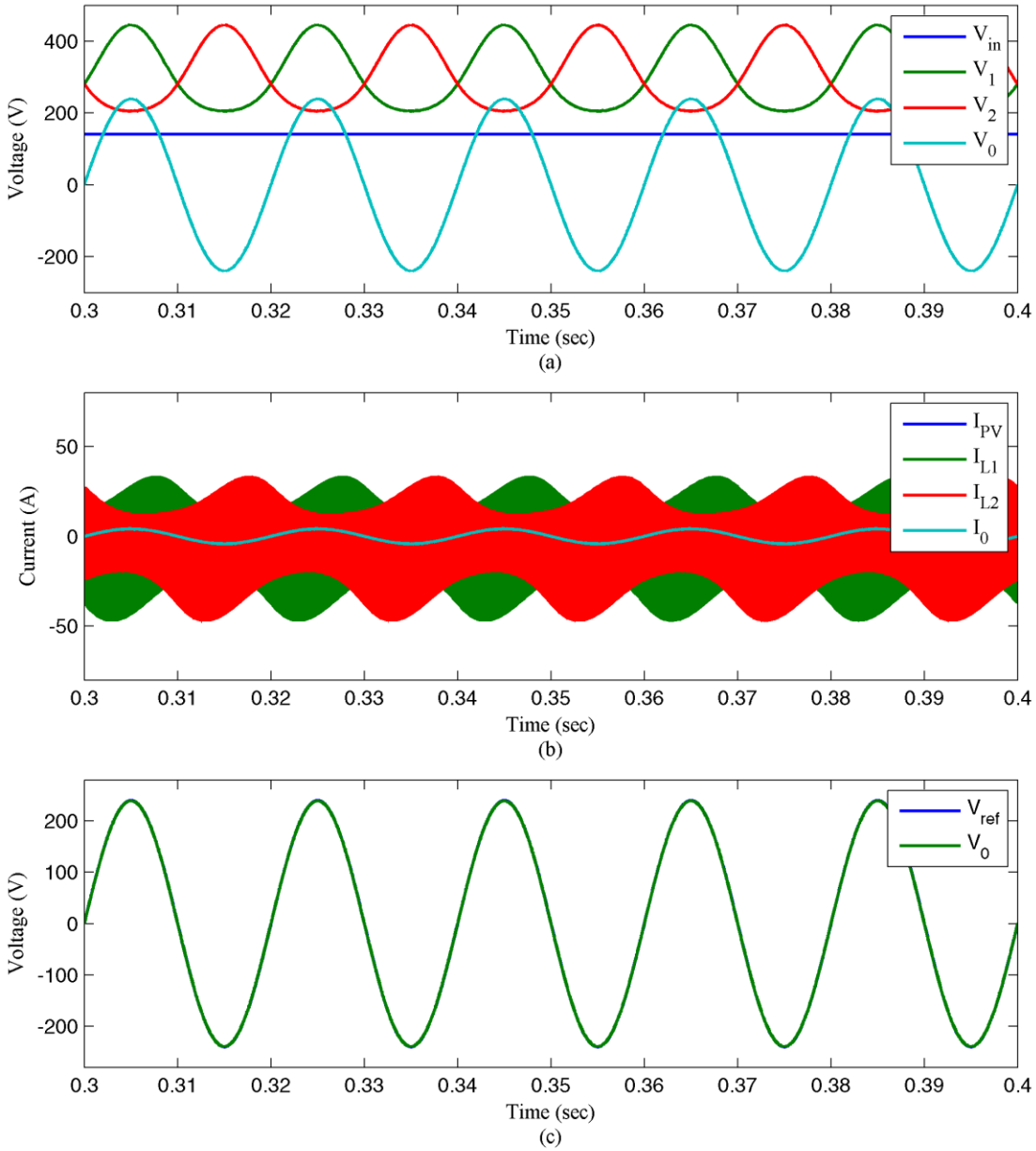


**Figure 11.** Normal operation of boost inverter controlled by MSOSMC under change in non-linear load. (a) PV voltage, capacitor voltages, output voltage, (b) PV current, inductor currents and load current (c) The comparison of output voltage with the reference voltage.

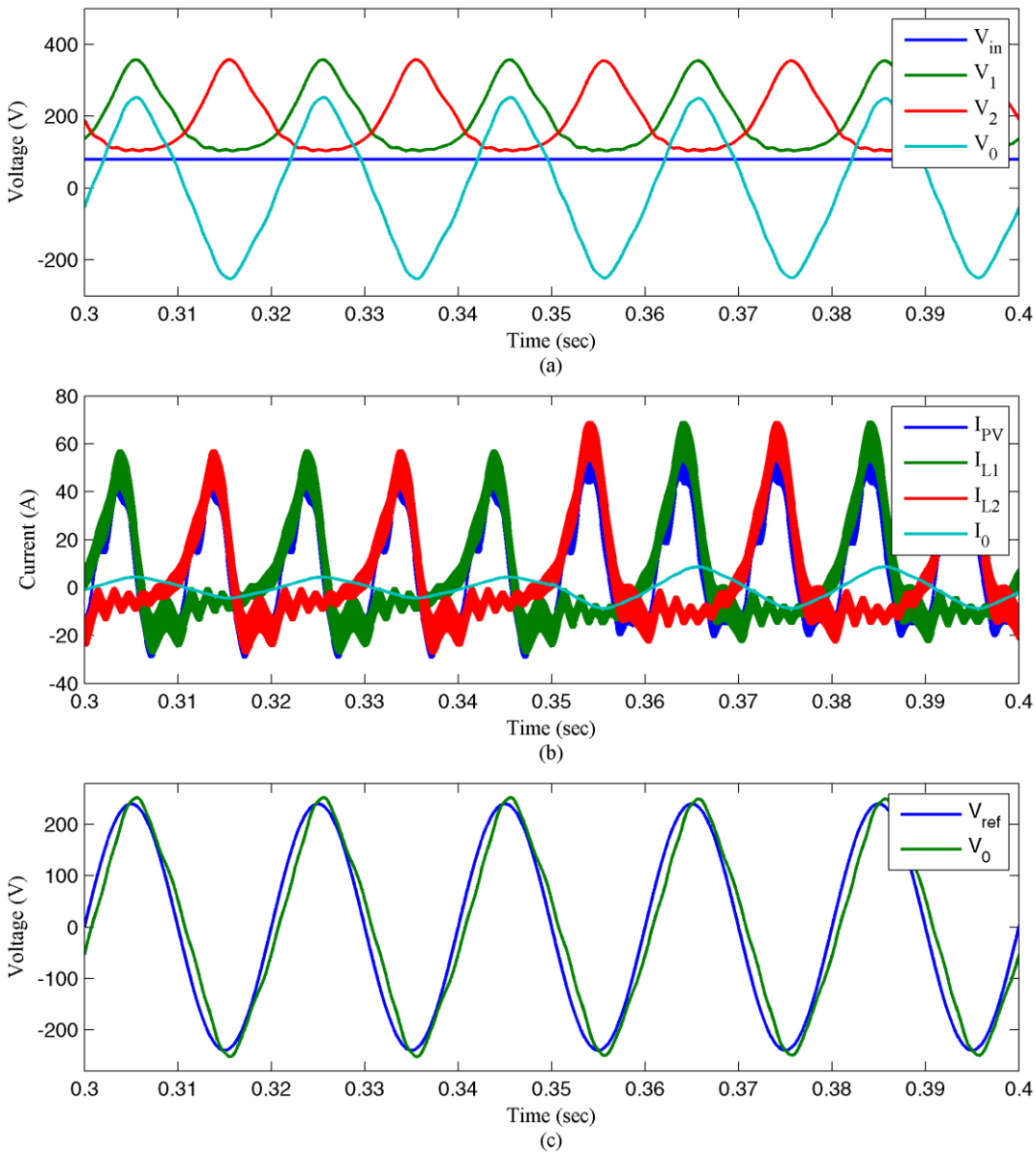


**Figure 12.** Normal operation of boost inverter controlled by DSMC under change in non-linear load. (a) PV voltage, capacitor voltages, output voltage, (b) PV current, inductor currents and load current (c) The comparison of output voltage with the reference voltage.

**Table 3.** Performance comparison of MSOSMC and DSMC methods.

| Conditions | Method | Power(W) | THD (%) |
|---|---|---|---|
| Nominal Performance | MSOSMC | 998 | 3.16 |
| | SMC | 998 | 7.73 |
| Irradiance variation $\lambda = 0.5$ to $1.0 kW/m^2$ | MSOSMC | 998 | 4.04 |
| | SMC | 995 | 11.96 |
| Load changed from 57.6 Ω to 28.8 Ω | MSOSMC | 998 | 3.25 |
| | SMC | 994 | 7.72 |
| Non-linear load R = 57.6 Ω to R = 57.6 Ω&100μH | MSOSMC | 895 | 3.68 |
| | SMC | 895 | 7.80 |

Table 3. summarizes the comparison between MSOSMC and DSMC. Both controllers are robust under parameter and load variations. But the THD is high in DSMC but less in MSOSMC. However, DSMC has ripples during input variation and load change but in case of MSOSMC, there is least ripple.

## CONCLUSIONS

This paper presents a MSOSMC for Boost Inverter in photovoltaic system. The sliding surface designed based on maximum power point voltage and sinusoidal output voltage in order to track voltage at maximum power point as well as reference sinusoidal voltage. A Lyapunov function is used to analysis the stability of the proposed controller. The performance of the closed loop control of boost inverter in PV system is verified in Matlab-Simulink. The proposed MSOSMC eliminates chattering caused by first order SMC and also ensures high efficiency under system imperfection. The proposed control technique is robustness under different weather and load conditions respectively. The proposed controller is compared with conventional SMC. The comparison result substantiates that the MSOSMC gives fast response, less chattering and low THD.

## REFERENCES

[1] S. Chatzivasileiadis, D. Ernst, and G. Andersson, 2013, "The Global Grid." Renewable Energy, 57, pp.372-383.

[2] P. D. Lund, 2009, "Effects of energy policies on industry expansion in renewable energy." Renewable Energy, 34(1), pp.53-64.

[3] J. Abushnaf and A. Rassau, 2018, "Impact of energy management system on the sizing of a grid-connected PV/Battery system." The Electricity Journal, 31(2),

pp.58-66.

[4] R. Dubey, D. Joshi, and R. C. Bansal, 2016, "Optimization of Solar Photovoltaic Plant and Economic Analysis." Electric Power Components and Systems, 44(18), pp.2025-2035.

[5] R. O. Caceres and I. Barbi, 1999, "A boost DC-AC converter: analysis, design, and experimentation." IEEE Transactions on Power Electronics, 14(1), pp.134-141.

[6] M. E. Şahin and H. İ. Okumuş, 2018, "Comparison of Different Controllers and Stability Analysis for Photovoltaic Powered Buck-Boost DC-DC Converter." Electric Power Components and Systems, 46(2), pp.149-161.

[7] P. Sanchis, A. Ursaea, E. Gubia, and L. Marroyo, 2005, "Boost DC-AC inverter: a new control strategy." IEEE Transactions on Power Electronics, 20(2), pp.343-353.

[8] R. Venkataramanan, 1986, "Sliding Mode Control of Power Converters." Ph.D. Thesis, California Institute of Technology, Pasadena, CA, USA.

[9] A. Kchaou, A. Naamane, Y. Koubaa, and N. M'sirdi, 2017, "Second order sliding mode-based MPPT control for photovoltaic applications." Solar Energy, 155, pp.758-769.

[10] B. B. Naik and A. J. Mehta, 2017, "Sliding mode controller with modified sliding function for DC-DC Buck Converter." ISA Transactions, 70, pp.279-287.

[11] K. Dahech, M. Allouche, T. Damak, and F. Tadeo, 2017, "Backstepping sliding mode control for maximum power point tracking of a photovoltaic system." Electric Power Systems Research, 143, pp.182-188.

[12] Y. Huangfu, S. Zhuo, K. A. Rathore, E. Breaz, B. Nahid-Mobarakeh, and F. Gao, 2016, "Super-Twisting Differentiator-Based High Order Sliding Mode Voltage Control Design for DC-DC Buck Converters." Energies, 9(7).

[13] D. B. W. Abeywardana, B. Hredzak, and V. G. Agelidis, 2017, "A Fixed-Frequency Sliding Mode Controller for a Boost-Inverter-Based Battery-Supercapacitor Hybrid Energy Storage System." IEEE Transactions on Power Electronics, 32(1), pp.668-680.

[14] B. Goldvin Sugirtha Dhas and S. N. Deepa, 2015, "Fuzzy logic based dynamic sliding mode control of boost inverter in photovoltaic application." Journal of Renewable and Sustainable Energy, 7(4), pp.043133.

[15] C. Albea, F. Gordillo, and C. Canudas-de-Wit, 2011, "Adaptive control design for a boost inverter." Control Engineering Practice, 19(1), pp.32-44.

[16] F. Flores-Bahamonde, H. Valderrama-Blavi, J. M. Bosque-Moncusi, G. García, and L. Martínez-Salamero, 2016, "Using the sliding-mode control approach for analysis and design of the boost inverter." IET Power Electronics, 9(8),

pp.1625-1634.

[17] G. R. Zhu, C. Y. Xiao, H. R. Wang, and S. C. Tan, 2016, "Closed-loop waveform control of boost inverter." IET Power Electronics, 9(9), pp.1808-1818.

[18] O. J. Moraka, P. S. Barendse, and M. A. Khan, 2015, "Dead time effect on the double loop control strategy for a boost inverter," 2015 IEEE Energy Conversion Congress and Exposition (ECCE), pp. 2498-2505, 2015.

[19] A. K. Pati and N. C. Sahoo, 2017, "Adaptive super-twisting sliding mode control for a three-phase single-stage grid-connected differential boost inverter based photovoltaic system." ISA Transactions, 69, pp.296-306.

[20] R. J. Wai, M. W. Chen, and Y. K. Liu, 2015, "Design of Adaptive Control and Fuzzy Neural Network Control for Single-Stage Boost Inverter." IEEE Transactions on Industrial Electronics, 62(9), pp.5434-5445.

[21] R. J. Wai, Y. F. Lin, and Y. K. Liu, 2015, "Design of Adaptive Fuzzy-Neural-Network Control for a Single-Stage Boost Inverter." IEEE Transactions on Power Electronics, 30(12), pp.7282-7298.

[22] D. B. W. Abeywardana, B. Hredzak, and V. G. Agelidis, 2015, "Single-Phase Grid-Connected LiFePO4 Battery - Supercapacitor Hybrid Energy Storage System With Interleaved Boost Inverter." IEEE Transactions on Power Electronics, 30(10), pp.5591-5604.

[23] M. M. Tahar, K. Zemalache Meguenni, and A. Omari, *High order sliding mode observer based backstepping control design for PWM AC/DC converter* vol. 16, 2016.

[24] M. Rezkallah, S. K. Sharma, A. Chandra, B. Singh, and D. R. Rousse, 2017, "Lyapunov Function and Sliding Mode Control Approach for the Solar-PV Grid Interface System." IEEE Transactions on Industrial Electronics, 64(1), pp.785-795.

[25] J. Liu, S. Laghrouche, and M. Wack, 2014, "Observer-based higher order sliding mode control of power factor in three-phase AC/DC converter for hybrid electric vehicle applications." International Journal of Control, 87(6), pp.1117-1130.

[26] I. de la Parra, M. Muñoz, E. Lorenzo, M. García, J. Marcos, and F. Martínez-Moreno, 2017, "PV performance modelling: A review in the light of quality assurance for large PV plants." Renewable and Sustainable Energy Reviews, 78, pp.780-797.

[27] K. Ishaque, Z. Salam, and Syafaruddin, 2011, "A comprehensive MATLAB Simulink PV system simulator with partial shading capability based on two-diode model." Solar Energy, 85(9), pp.2217-2227.

[28] C. L. Trujillo, F. Santamaría, and E. E. Gaona, 2016, "Modeling and testing of two-stage grid-connected photovoltaic micro-inverters." Renewable Energy,

99, pp.533-542.

[29] A. Pandey, N. Dasgupta, and A. K. Mukerjee, 2008, "High-Performance Algorithms for Drift Avoidance and Fast Tracking in Solar MPPT System." IEEE Transactions on Energy Conversion, 23(2), pp.681-689.

[30] G. Bartolini, A. Ferrara, and E. Usai, 1998, "Chattering avoidance by second-order sliding mode control." IEEE Transactions on Automatic Control, 43(2), pp.241-246.

[31] D. Cortes, N. Vazquez, and J. Alvarez-Gallegos, 2009, "Dynamical Sliding-Mode Control of the Boost Inverter." IEEE Transactions on Industrial Electronics, 56(9), pp.3467-3476.